

NANOSILICA-REINFORCED POLYMER COMPOSITES

POLIMERNI KOMPOZITI OJAČANI Z NANOSILIKO

Marjetka Conradi

Institute of Metals and Technology, Lepi pot 11, 1000 Ljubljana, Slovenia
marjetka.conradi@imt.si

Prejem rokopisa – received: 2013-02-28; sprejem za objavo – accepted for publication: 2013-03-07

In the fast growing field of nanotechnology, polymer nanocomposites have become a prominent area of current research and development. Silica/polymer nanocomposites are dominating the polymer and composite literature as well as a variety of applications, many industrial products and other significant areas of current and emerging interest. This review will give a general overview of the leading and most commonly used techniques and strategies for the preparation of both silica fillers and silica/polymer nanocomposites, followed by a discussion of the main characterization methods, mechanical testing, properties and applications. Typical examples of different systems will be reported and referred to the corresponding references for more detailed descriptions.

Keywords: nanosilica, polymers, composites

V sklopu hitro razvijajoče se panoge, imenovane nanotehnologija, so dobili polimerni nanokompoziti pomembno vlogo na področju raziskav in razvoja. Polimerni silicijevi dioksidni nanokompoziti dominirajo tako v literaturi, namenjeni raziskavam polimerov in kompozitov, kot tudi v številnih aplikacijah ter industrijskih produktih. V tem preglednem članku se bomo osredinili na splošni pregled vodilnih in najpogosteje uporabljenih tehnik ter strategij za pripravo tako silicijevih vključkov kot tudi polimernih silicijevih dioksidnih nanokompozitov. Sledila bo razprava o glavnih metodah karakterizacije silika/polimernih nanokompozitov, mehanskih preizkusov, o lastnostih ter njihovih aplikacijah. Predstavljeni bodo primeri različnih polimernih silicijevih dioksidnih kompozitnih sistemov skupaj z ustreznimi referencami za podrobnejši vpogled.

Ključne besede: nano silicijev dioksid, polimeri, kompoziti

1 INTRODUCTION

Polymer (nano)composites have been extensively studied over a long period of time. They are generally organic polymer composites mostly filled with inorganic fillers. Their properties combine the advantages of the inorganic filler material (i. e., rigidity, thermal stability) and of the organic polymer (i. e., flexibility, ductility, processability). However, the main advantage of these composites is characterized by the volume fraction and size of the fillers. If the fillers decrease in size from the micro- to the nanoscopic scale, unique properties of polymer nanocomposites are emphasized as the small size of the fillers leads to a dramatic increase in the interfacial area as compared with the ordinary composites. This interfacial area then creates a significant volume fraction of the interfacial polymer with the properties different from the bulk polymer even at low filler loadings.^{1,2}

Reinforcement agents such as glass particles,^{3,4} ceramic particles,⁵ layered silicates,⁶⁻⁸ metal particles,⁹ rubber plastics¹⁰ and thermoplastics^{11,12} have already been successfully used. Several researchers have studied the effects of the particle size and volume fraction on the mechanical response of polymer composites.¹³⁻¹⁷ There are a few analytical models based on the crack propagation along the particle surfaces taking the interspacing between the particles into account¹⁸ as well as mathematically considered trapping, pinning and bridging of the crack front on the particles.¹⁹⁻²¹ It has been shown

that the fracture phenomena of the composites filled with nanometer-sized particles differ from the behaviour of the composites filled with micrometer-sized or larger filler particles.

However, among the numerous polymer composites, silica/polymer nanocomposites are the most commonly reported in the literature and are also employed in a variety of applications, such as electronics, automotive and aerospace industries as well as used in many industrial products due to their good mechanical characteristics²². In order to further improve the properties of silica/polymer nanocomposites, their preparation, characterization, mechanical properties and applications have become quickly expanding fields of research in the past few years.

The aim of this review is to give a general overview of the leading and most commonly used techniques and strategies for the preparation of both silica fillers and nanosilica/polymer composites, followed by a short discussion of the main characterization methods, mechanical testing, properties and applications. Typical examples of different systems are reported and referred to the corresponding references for more detailed descriptions.

2 PREPARATION OF SILICA FILLERS

Silica particles normally exist in a form of a fine, white amorphous powder or colloid suspension. Its most

important characteristic is an extremely large surface area and a smooth nonporous surface, which can promote a strong physical contact when embedded in a polymer matrix.

Nowadays silica particles are commercially available in all sizes ranging from nanometer to micrometer; however, several researchers still synthesize particles on their own. Two main methods have been developed for silica-particle formation: the sol-gel method and the microemulsion method.²³ In 1968, however, Stöber and Fink²⁴ introduced a simple synthesis of monodisperse spherical silica particles starting with tetraethyl orthosilicate (TEOS 98 %), deionized water, ammonia (25 %) and absolute ethanol (99.9 %) as the alkoxide precursor, hydrolyzing agent, catalyst and solvent. In the process, two mother solutions are prepared, one containing ammonia-water, and the other containing TEOS-ethanol. The two solutions are mixed in a thermostatically controlled water bath (50 ± 1) °C. After 60 min, the resulting spheres are separated from the liquid phase with centrifugation and then ultrasonically dispersed in deionized water. Finally, the particles can be dried in an oven at 50 °C to obtain white powder. Note that using this method, the final particle size critically depends on the reagent concentrations, molar ratio and reaction temperature. As shown in **Figure 1** good monodispersity of silica spheres can be obtained with this method.²⁵

The dispersion of silica fillers and, consequently, the compatibility between the polymer and silica have a crucial impact on the mechanical properties of silica/

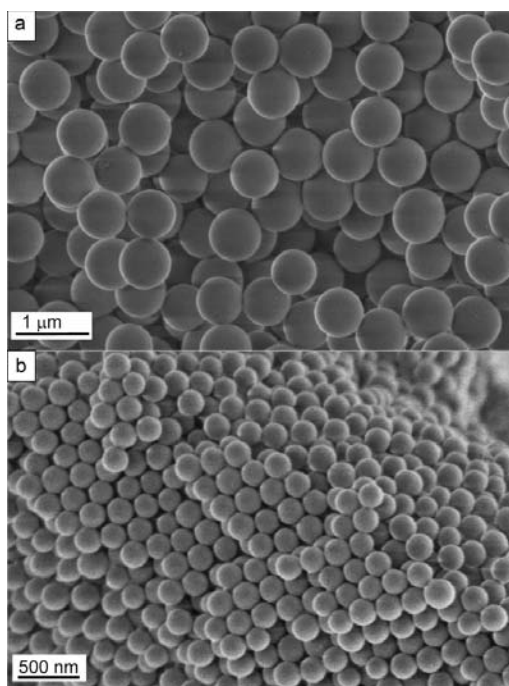


Figure 1: Scanning electron microscopy (SEM) images of SiO₂ particles prepared according to the Stöber procedure, a) 650 nm silica particles, b) 240 nm silica particles²⁵

Slika 1: SEM-slika SiO₂ delcev, sintetiziranih po metodi Stöberja, a) silicijevi delci 650 nm, b) silicijevi delci 240 nm²⁵

polymer composites. As most of the polymers are hydrophobic in nature, it is important to improve the interfacial interaction between the matrix and silica via silica-surface modification, which can also improve its dispersion in the matrix at the same time. In general, the surface of silica fillers can be successfully modified with either chemical or physical methods.

Modification of silica via a chemical interaction involves a modification of its surface with modifying agents (i. e., silanes) or grafting polymers. The most common way of making silica hydrophobic and polymer compatible, is silanization. We can find a long list of silane coupling agents that generally have hydrolysable and organofunctional ends and can be represented as RSiX₃. X stands for hydrolysable groups, typically chloro, methoxy or ethoxy groups, and R stands for the organo group that has to be chosen according to the properties of the polymer. Silanes are attached to the silica surface through the reaction of hydrolysable groups with the hydroxyl groups on the silica surface while the alkyl chains interact with the polymer²⁶ (**Figure 2**).

Hydrophobicity, on the other hand, can be successfully increased by grafting the polymer chains to silica particles either with a covalent attachment of end-functionalized polymers to the surface or with an in-situ monomer polymerization.

If silica is modified via a physical interaction, the procedure usually involves surfactants or macromolecules adsorbed onto its surface. In principle, a polar group of surfactants is adsorbed to the surface of silica by an electrostatic interaction. As a consequence, the physical attraction between the silica particles within agglomerates is reduced, making silica particles easy to incorporate into a polymer matrix.²⁷

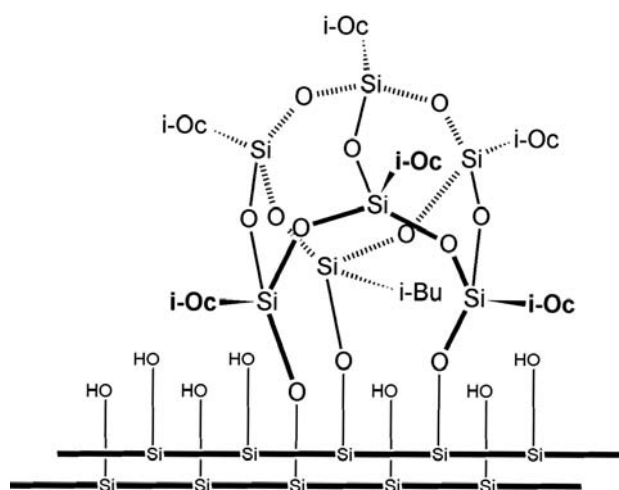


Figure 2: Schematic presentation of the silica-surface modification by trisilanol heptaisobutyl silesquioxane (IB₅(SiO_{3/2})₈(OH)₃) via a covalent bonding²⁶

Slika 2: Shematski prikaz modifikacije silicijeve površine s trisilanol heptaisobutil sileskvioksanom (IB₅(SiO_{3/2})₈(OH)₃) na osnovi kovalentne vezi²⁶

3 COMPOSITE PREPARATION

The main concern in composite preparation is the mixing process and the obtained homogeneous silica dispersion in the polymer matrix. Therefore, prior to the composite preparation, the compatibility between the two components has to be assured to avoid silica agglomeration, using one of the methods described in the previous section.

The simplest method of silica/polymer composite preparation is direct mixing of silica into the polymer matrix, i. e., by melt or solution blending. Besides blending, sol-gel processes and in-situ polymerization are also widely used among the preparation techniques.

3.1 Blending

Melt blending is the most commonly used method in composite preparation due to its efficiency and operability. In the process, the polymer and the inorganic filler (i. e., silica) are sheared in the melt at a temperature equal or greater than the melting point of the polymer. Under suitable conditions the material exfoliates and disperses to the desired extent. This technology is very versatile and can be applied to various polymers.^{28–31} It is also possible to add swelling and compatibilizing agents in order to improve the exfoliation and reach a better adhesion between the two major components.

Solution blending, on the other hand, is a liquid-state powder-processing method that allows a good molecular level of mixing. Solution blending can be achieved by either dissolving only the polymer matrix or dissolving both the matrix and the nanoparticles.

3.2 Sol-gel process

The sol-gel process is a synthesis route consisting of the preparation of a sol, the successive gelation and the solvent removal. Within the past decades sol-gel processes have been widely used to synthesize novel organic/inorganic composite materials. In the case of composites, the goal is to carry out the sol-gel reaction in the presence of polymeric molecules (i.e., the organic phase) containing functional groups that improve their bonding to the inorganic phase. This is a very successful reinforcement technique that can generate filler particles within a polymer matrix.

3.3 In-situ polymerization

In-situ polymerization is a very effective and fast way to construct a nanocomposite material. In this method, the fillers are first pretreated with appropriate surface modifiers and then added directly to the liquid monomer during the polymerization stage. Using the solution method, fillers are added to a polymer solution using solvents such as toluene, chloroform and acetonitrile to integrate the polymer and filler molecules.

4 CHARACTERIZATION

A homogeneous distribution of finely dispersed fillers in a silica/polymer composite is a prerequisite for obtaining good mechanical properties of the end material. In a composite, interfacial interaction between the fillers and the polymer matrix plays a crucial role in toughening the composite. In order to achieve a high particle/polymer area and to distribute the mechanical stresses within the composite, the composite has to consist of homogeneously distributed filler particles which are not agglomerated. Therefore, prior to further mechanical testing, the chemical structure, morphology and microstructure of the composites must be analysed.

4.1 Infrared and Raman spectroscopy

Infrared and Raman spectroscopy are normally used to confirm the surface modification of the silica fillers implemented in a polymer matrix. Building up a modifier layer around the silica particles can be followed by inspecting the spectra of the filler^{32,33} or the vibrational bands of the surface modifier, the intensities of which depend on the number of the filler surface sites occupied by the modifier.

In **Figure 3**, typical IR transmission spectra of the silica-surface modifier trisilanol (IO₇) POSS, polymer polyvinyl chloride (PVC), 30 nm silica/PVC and 130 nm silica/PVC composites are presented.³⁴ The silanol groups of open-cage POSS do not spontaneously lead to condensation, as silanols of other simple alkoxy silanes, but preferentially interact with the active sites on the surface of the filler.³⁵ Normally, the bands attributed to trisilanol POSS are weak because the Si-O-Si bands are covered by the same band of silica spheres. However, a closer inspection of the peak intensity of the band at 2907 and 2953 cm⁻¹ indicates a progressive occupation of the accessible sites on the silica surface. A comparison of the infrared spectra in the C-H region of trisilanol POSS (**Figure 3** zoom), modified silica/PVC

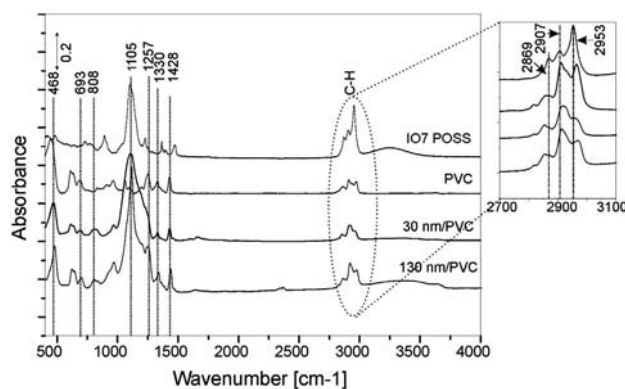


Figure 3: IR transmission spectra of trisilanol (IO₇) POSS, PVC, 30 nm silica/PVC and 130 nm silica/PVC composites³⁴

Slika 3: IR-transmisijski spektri trisilanola (IO₇) POSS, PVC-ja, kompozitov silicijev dioksid-PVC 30 nm in silicijev dioksid-PVC 130 nm³⁴

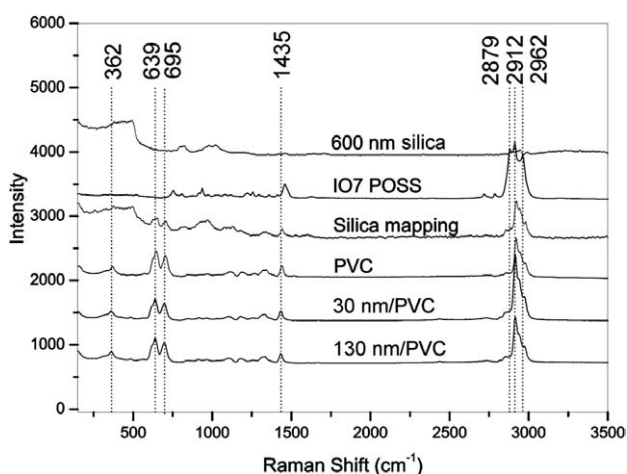


Figure 4: Raman spectra of pure 600 nm silica spheres, trisilanol (IO_7) POSS, the average spectrum of silica mapping, pure PVC, 130 nm silica/PVC and 30 nm silica/PVC composites³⁴

Slika 4: Ramanski spektri neobdelanih 600 nm silicijevih delcev, trisilanola (IO_7) POSS, povprečnega spektra silicijevega mapiranja čistega PVCja ter 130 nm silika/PVC in 30 nm silika/PVC kompozitov³⁴

composite and bulk PVC revealed the presence of trisilanol POSS on the silica surface. The C-H band at 2953 cm^{-1} was also present in the spectrum of the bulk PVC and could be seen in the spectrum of the PVC composite as well. Surprisingly, the C-H band at 2907 cm^{-1} surpasses the band at 2953 cm^{-1} because of the presence of isooctyl groups on the surface.

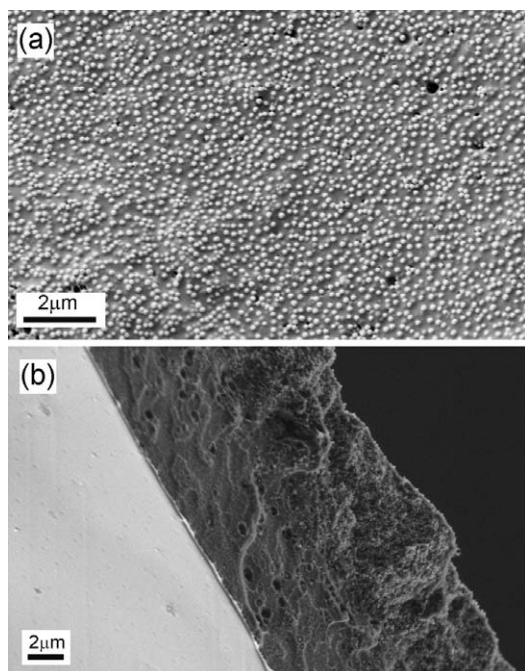


Figure 5: a) Top-view and b) side-view SEM micrographs of a silica/PVC composite composed of volume fraction 30 % of POSS-silanated, 130 nm silica fillers³⁴

Slika 5: SEM-pogled: a) z vrha in b) pogled s strani kompozitov silicijev dioksid-PVC, sestavljenih iz volumenskega deleža 30 % POSS-silaniziranih silicijevih dioksidnih vključkov 130 nm³⁴

In **Figure 4** typical Raman spectra of composite silica/PVC recorded as a function of the size of silica spheres is presented. In the Raman spectrum of PVC, polarized lines are observed at 639, 695, and 1435 cm^{-1} . The band at 1435 cm^{-1} is assigned to the CH_2 scissors vibration and a broad doublet-like band envelope in the region of $600\text{--}700\text{ cm}^{-1}$ was attributed to C-Cl stretching vibrations.³⁶ For comparison, we recorded the Raman spectrum of pure, bulk, 600 nm silica spheres, which have a very weak response in the fingerprint range (i.e., $500\text{--}2000\text{ cm}^{-1}$) and also in the CH region. Inside the composites under investigation, we, therefore, used the mapping of silica spheres. The average spectrum of silica mapping in **Figure 4** indicates a modification of the silica spheres as the spectrum includes the bands of pure silica and the bands of trisilanol IO_7 POSS. In addition, PVC has a similar response in the CH region. A successful modification of 30 nm silica/PVC and 130 nm silica/PVC composites was further identified with an elevated band at 2912 cm^{-1} . This band reveals the isooctyl structure of POSS mostly because the other bands are not so strong in the Raman spectra.

4.2 Scanning electron microscopy and transmission electron microscopy

Scanning electron microscopy (SEM) and transmission electron microscopy (TEM) are the most common methods used in the morphology evaluation.

In **Figure 5** we see typical SEM micrographs of POSS-silanated, 130 nm silica/PVC composites. We can see that a 130 nm silica/PVC composite consisted of 3D-ordered silica particles. SEM micrographs also revealed (**Figure 5b**) that the 3D silica-particle structure was ousted towards the film surface, frequently encountered with polymers consisting of two phases with a poor mutual compatibility due to their different chemical compositions. Typical examples are polymers with a low surface energy obtained with an addition of fluoropolymers or fluorosilanes.³⁷

Another example of SEM imaging in composite-morphology characterization is an analysis of the fracture surface of a composite filled with a very low amount of silica fillers, i.e., less than volume fraction 1 %. Due to the small amount of silica fillers it is not possible to observe isolated particles or an arrangement of particles as shown previously in **Figure 5**; however, the information on the particle inclusion can be revealed with an analysis of the properties of fracture surfaces.

In **Figure 6** typical fracture surfaces of the neat epoxy and diglycidyl ether of bisphenol A surface-treated, 30-nm and 130-nm silica/epoxy composites are presented.³⁸ Prior to the SEM imaging the samples were frozen in liquid nitrogen and broken by hand in order to observe the natural crack propagation in the composite. The inclusion of silica fillers in the epoxy matrix is confirmed by an increased roughness of the composite's

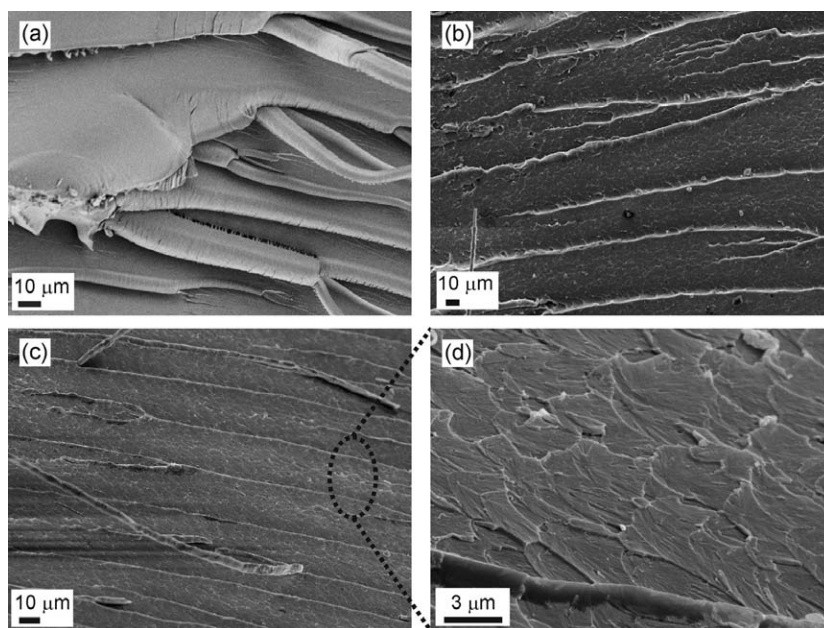


Figure 6: a) Hand broken fracture surfaces of pure epoxy, b) composite with the volume fraction 0.5 % diglycidyl ether of bisphenol A surface-treated, 30-nm silica fillers, c) composite with 0.5 % diglycidyl ether of bisphenol A surface-treated, 130-nm silica fillers and d) a fracture surface detail – a fish-skin-like microstructure – of the 130-nm silica/epoxy composite³⁸

Slika 6: a) Lomna površina vzorcev čistega epoxyja, b) kompozita, obogatenega z volumenskim deležem 0,5 % z diglicidil etrom bisfenola A površinsko obdelanih 30-nm silicijevih vključkov, c) kompozita, obogatenega z volumenskim deležem 0,5 % z diglicidil etrom bisfenola A površinsko obdelanih silicijevih dioksidnih vključkov 130 nm in d) detajl lomne površine – mikrostruktura ribje kože v kompozitu silicijev dioksid-epoksi 130 nm³⁸

fracture surface as compared to the smooth surface of the pure epoxy. Both silica and epoxy composites break in sharp fracture lines and characteristic steps decorated with a fish-skin-like microstructure (**Figure 6d**) that also indicates an increased brittleness compared to the pure epoxy. The roughness of the fracture surface, however, slightly decreased with the decreasing particle size.

Transmission electron microscopy can serve as a very useful tool for determining the exact size and distribution of the embedded nanoparticles. In **Figure 7** a typical micrograph of the metal nanoparticles embedded in a polymer matrix is presented.

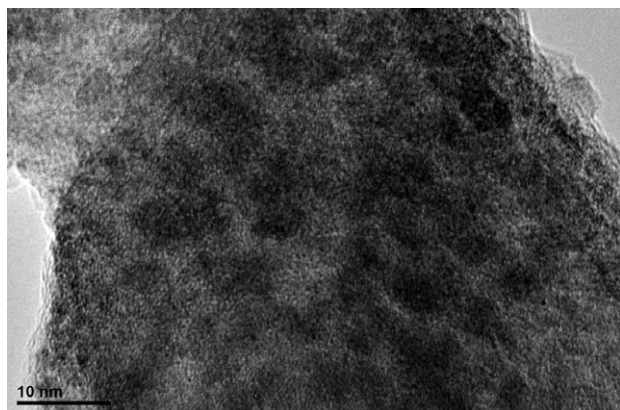


Figure 7: TEM micrograph of the Fe₂O₃ nanoparticles embedded in the polypropylene (PP) matrix

Slika 7: TEM-slika Fe₂O₃ nanodelcev v mreži polipropilena (PP)

5 MECHANICAL PROPERTIES

One of the primary reasons for adding inorganic fillers to polymers is to improve their mechanical performance through optimization of the balance between the strength/stiffness and the toughness of a composite. The mechanical response of composites strongly depends also on the silica content and size and is generally characterized with respect to different properties, such as the tensile strength, flexural strength, hardness, impact strength, fracture toughness, etc.

5.1 Tensile-strength test

With the tensile test we analyse stress σ and strain ε that are determined from the measured load and deflection using the original specimen cross-sectional area S_0 and length l_0 as follows:

$$\sigma = F/S_0, \varepsilon = d/l/l_0$$

Typical stress-strain curves of pure PVC and POSS-silanated silica/PVC composites with two types of silica fillers, 130 nm and 30 nm in diameter, are summarized in **Figure 8**. For silica/PVC composites, the trend reported in **Figure 8** can be divided into four stages before the material breaks: the initial linear elasticity, nonlinear transition to global yield, region of necking and strain softening. However, the stress-strain behaviour of pure PVC is different, typically with a broad constant stress regime for increasing the strain without a pro-

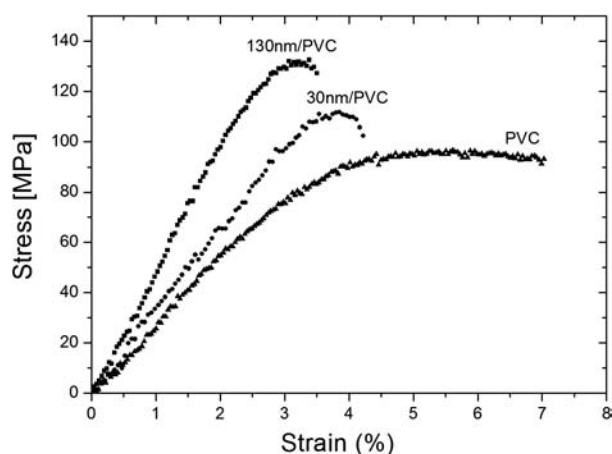


Figure 8: Typical stress-strain diagram for pure PVC and silica/PVC composites with POSS-silanated, 130 nm and 30 nm silica fillers as obtained with the tensile-strength test³⁴

Slika 8: Z nateznim preizkusom dobljen značilen diagram napetost-deformacija čistega PVCja in kompozitov silicijev dioksid-PVC, obogatenih s POSS-silaniziranimi 130 nm in 30 nm silicijevimi dioksidnimi vključki³⁴

nounced necking or strain softening before the sample breaking.

In the low strain portion of the curves all the investigated samples followed Hooke's law giving us the information on the composite modulus of elasticity E . As shown in **Table 1**, we observed a 30–40 % increase in E , making 30 nm and 130 nm silica/PVC composites stiffer. This large increase in elastic modulus is due to a large amount of silica particles. Another material proportion that we can obtain from the stress-strain diagram is the maximum tensile strength (UTS). A significant strengthening is observed in both 30 nm and 130 nm silica/PVC composites, 20–30 %, respectively (**Table 1**). An opposite response is, however, observed for the elongation at break depending on the silica size in the PVC matrix (**Table 1**). In contrast to the increased stiffness of 30 nm and 130 nm silica/PVC composites, their elongation at break that is lower than for pure PVC (15–30 %) indicates an embrittlement effect upon an addition of silica fillers.

5.2 Three-point bending test

The three-point bending test (3PB) covers the determination of flexural properties of a material by measuring the deflection of a sample under applied load. **Figure 9** shows a typical stress-strain curve for the samples under investigation, diglycidyl ether of bisphenol A surface-treated silica composites and the neat epoxy. **Table 2** lists the corresponding material proportions obtained with the 3PB test: elastic modulus (E), maximum tensile strength (UTS) and elongation at break.

We observed an approximately 10–20 % increase in E and UTS for both composites compared to the pure epoxy. The experimental scattering of both the Young's

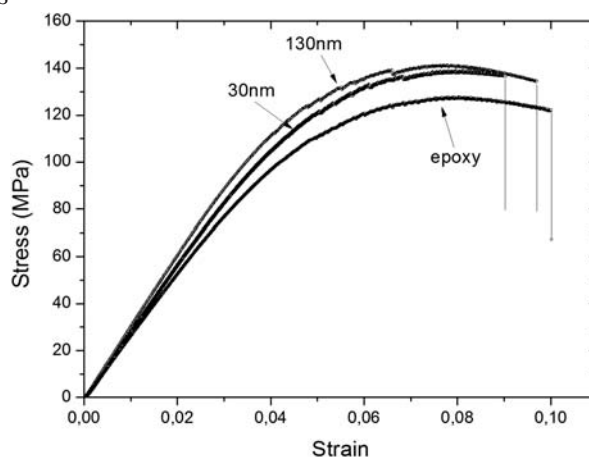


Figure 9: Typical stress-strain curves of diglycidyl ether of bisphenol A surface-treated silica/epoxy composites and the neat epoxy as obtained with the 3PB test³⁸

Slika 9: Z upogibnim preizkusom (3PB) dobljen značilen diagram napetost – deformacija z diglicidil etrom bisfenola A silaniziranih kompozitov silicijevga dioksida-epoksi in čistega epoksija³⁸

Table 1: Elastic modulus (E), tensile strength (UTS) and elongation at break of POSS-silanated silica/PVC composites and pure PVC evaluated with the tensile test³⁴

Tabela 1: Z nateznim preizkusom dobljen elastični modul (E), maksimalna natezna trdnost (UTS) in raztezek pri pretrgu POSS-silaniziranih kompozitov silicijev dioksid-PVC in čistega PVC³⁴

Sample	E /GPa	UTS/MPa	elongation at break (%)
PVC	1.7	89.9	7.0
PVC + 60 % vol. fractions of SiO ₂ 30 nm	2.4	112.1	6.0
PVC + 60 % vol. fractions of SiO ₂ 130 nm	3.0	122.2	4.9

Table 2: Elastic modulus (E), tensile strength (UTS) and elongation at break of diglycidyl ether of bisphenol A surface-treated silica/epoxy composites and the neat epoxy evaluated with the 3PB test³⁸

Tabela 2: Z upogibnim preizkusom (3PB) dobljen elastični modul (E), maksimalna natezna trdnost (UTS) in raztezek pri pretrgu z diglicidil etrom bisfenola A silaniziranih kompozitov silicijev dioksid-epoksi in čistega epoksija³⁸

Sample	E /GPa	UTS/MPa	elongation at break (%)
Epoxy	2.6	127	10.0
Epoxy + 0,5 % vol. fractions of SiO ₂ 130 nm	3.0	141	9.6
Epoxy + 0,5 % vol. fractions of SiO ₂ 30 nm	2.8	138	9.0

modulus and the UTS was less than 10 %. The incorporation of silica fillers, on the other hand, caused a decrease in the elongation at break, which implies an increase in the composite brittleness.

5.3 Fracture toughness

The fracture-toughness test is designed to characterize the toughness of a material in terms of the critical-stress-intensity factor, K_{IC} , and the energy per unit area of a crack surface or the critical strain energy

release rate, G_{IC} , at the fracture initiation. In the experiment, the load-deflection curves are measured as shown in **Figure 10**. The fracture toughness, K_{IC} , is then calculated by using linear elastic fracture mechanics:³⁹

$$K_{IC} = \frac{SP_c}{BW^{3/2}} f(\xi)$$

where

$$f(\xi) = \frac{3\xi^{1/2} \{1.99 - \xi(1-\xi)(215 - 3.93\xi + 2.7\xi^2)\}}{2(1+2\xi)(1-\xi)^{3/2}}$$

$$\xi = \frac{a_0}{W}$$

S and P_c are the span length and the maximum load; B , W and a_0 are the thickness, the width and the pre-crack length of the specimen.

In **Figure 10** diglycidyl ether of bisphenol A surface-treated silica composites and the neat epoxy show a linear response until the brittle fracture occurs. The extracted experimental results for the fracture toughness, K_{IC} , for the composites and the neat epoxy are listed in **Table 3**, showing a fracture toughness increase by 25–30 % with the addition of silica fillers.

Table 3: Fracture toughness of diglycidyl ether of bisphenol A surface-treated silica composites and the neat epoxy³⁸

Tabela 3: Lomna žilavost z diglicidil etrom bisfenola A silaniziranih kompozitov silicijev dioksid-epoksi in čistega epoksija³⁸

Sample	$K_{IC}/(\text{MPa m}^{1/2})$
Epoxy	0.66 ± 0.05
Epoxy + 0.5 % vol. fractions of SiO_2 130 nm	0.91 ± 0.06
Epoxy + 0.5 % vol. fractions of SiO_2 30 nm	0.93 ± 0.06

5.4 Charpy impact strength test

The Charpy test is used to evaluate the amount of absorbed energy by a material during a fracture, there-

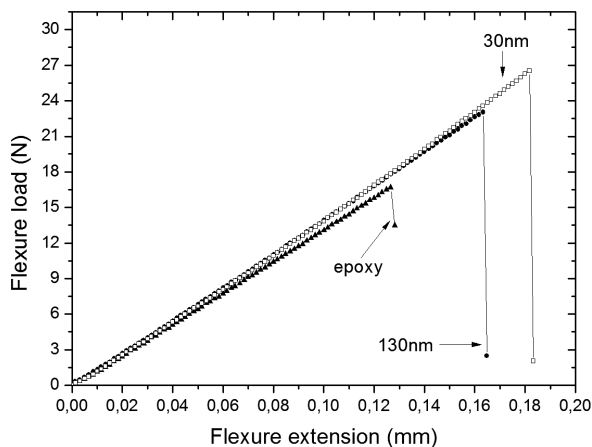


Figure 10: Load-deflection curves of diglycidyl ether of bisphenol A surface-treated silica composites and the neat epoxy³⁸

Slika 10: Diagram sila – deformacija z diglicidil etrom bisfenola A silaniziranih kompozitov silicijev dioksid-epoksi in čistega epoksija³⁸

fore giving us information on the impact toughness of the material. An example of the Charpy impact strength test results is in **Table 4**, presenting the impact energy and the impact resistance for diglycidyl ether of bisphenol A surface-treated silica composites and the neat epoxy.

Table 4: Impact energy and impact resistance of diglycidyl ether of bisphenol A surface-treated silica composites and the neat epoxy³⁸

Tabela 4: Energija pri prelomu in odpornost proti prelomu z diglicidil etrom bisfenola A silaniziranih kompozitov silicijevega dioksida-epoksi in čistega epoksija³⁸

Sample	Impact energy E_{imp}/J	Impact resistance $R_{imp}/(\text{kJ}/\text{m}^2)$
Epoxy	0.19 ± 0.02	6.4 ± 0.7
Epoxy + 0.5 % vol. fractions of SiO_2 130 nm	0.26 ± 0.02	8.9 ± 0.6
Epoxy + 0.5 % vol. fractions of SiO_2 30 nm	0.33 ± 0.03	10.8 ± 0.7

The addition of silica particles increases the impact resistance as well as the impact energy up to 60 %. Surprisingly, the results of the Charpy impact test are also strongly influenced by a particle diameter.

6 APPLICATIONS

As shown earlier, nanosilica-reinforced polymer composites significantly improve the mechanical pro-

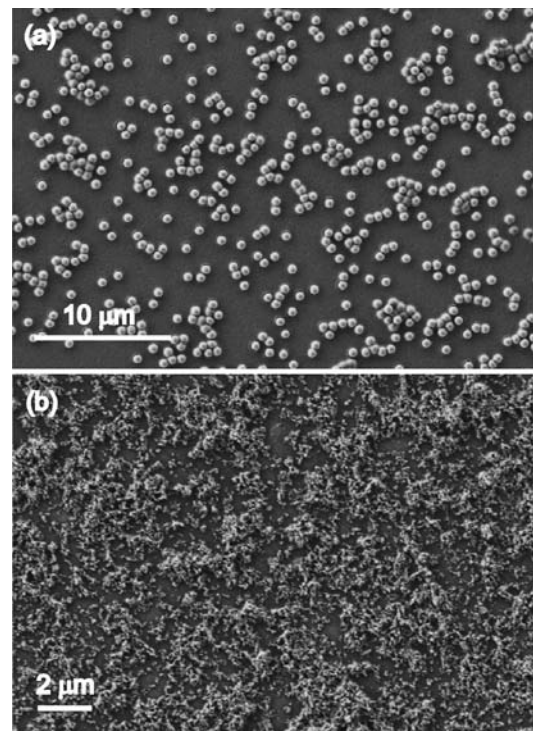


Figure 11: SEM micrographs of POSS-silanated, a) 600 nm and b) 30 nm silica/PVC composite coatings on the AISI 316L surface⁴⁵

Slika 11: SEM-slike POSS-silaniziranih kompozitnih prevlek silicijevega dioksida-PVC a) 600 nm in b) 30 nm na površini AISI 316L jekla⁴⁵

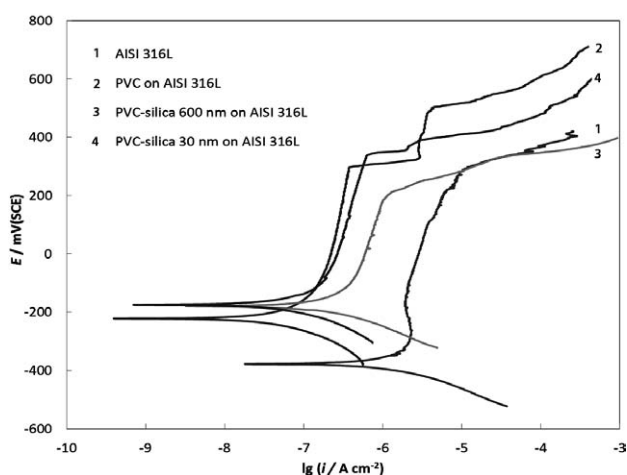


Figure 12: Potentiodynamic curves for AISI 316L, AISI 316L + PVC, AISI 316L + 600 nm/PVC and AISI 316L + 30 nm/PVC in 3.5 % NaCl⁴⁵

Slika 12: Potenciodinamske krivulje vzorcev AISI 316L, AISI 316L + PVC, AISI 316L + 600 nm/PVC in AISI 316L + 30 nm/PVC v 3,5-odstotni NaCl⁴⁵

properties of the end material and exhibit some unique properties allowing many potential applications. Silica/polymer nanocomposites have been reported to be used in coatings,^{40,41} optical devices,⁴² electronics,⁴³ photoresist materials,⁴⁴ etc.

In most cases silica/polymer nanocomposites are used as protective coatings, either to improve the mechanical characteristics of the substrate material (i. e., wear, scratch, abrasion resistance) or to insure the corrosion resistance in various environments. Corrosion-protection nanosilica/polymer coatings on metallic substrates, for example, provide an effective physical barrier between the metal and its environment containing aggressive species, such as enhanced chloride-ion concentration, O₂ or H⁺. A uniform dispersion of nanoparticles (i.e., SiO₂) in a chosen polymer matrix with desirable characteristics (i. e., epoxy) is shown to increase the surface hydrophobicity (i.e., the self-cleaning effect) and to improve the adhesion between the composite coating and the metallic surface.^{26,45–47}

In **Figures 11a** and **b** we can see an example of a POSS-silanated silica/PVC coating adsorbed on a steel substrate of type AISI 316L. **Figure 12** further presents potentiodynamic measurements of these coatings in a 3.5 % NaCl solution at room temperature indicating an improved anticorrosion behaviour in a chloride-ion-rich environment as compared to the clean AISI 316L surface. Potentiodynamic curves reflect the decreased corrosion-current densities and corrosion potentials for the silica/PVC-coated AISI 316L substrates.

7 SUMMARY AND OUTLOOK

A modification of a polymer matrix with silica fillers allows significant increases in the modulus and strength

contributions of the matrix to the overall composite properties. Obtaining the optimum properties for the nanocomposites, however, requires an excellent homogeneous dispersion of the fillers, as the tendency of the silica particles to agglomerate can seriously affect the achievable properties. Therefore, to provide a strong interfacial interaction between the inorganic particles and the polymer matrix, silica fillers must have suitably modified surfaces. The end result is a composite with unique and significantly improved mechanical properties having a high ability to transfer the stresses from the polymer matrix to the embedded particles. This allows the silica/polymer nanocomposites to be used in a variety of applications and industrial products successfully replacing the classical materials. Although much work has already been done on the silica/polymer nanocomposites, more research is needed to further understand the complex filler-matrix relationship that would allow a step forward and even enable a synthesis of the nanocomposites with controllable properties through tailoring the interfacial interaction between silica and a polymer matrix.

Acknowledgement

The author gratefully acknowledges the Slovenian programme P2-0132, "Fizika in kemija površin kovinskih materialov" of the Slovenian Research Agency for its support.

8 REFERENCES

- 1 A. C. Balazs, T. Emrick, T. P. Russell, Nanoparticle polymer composites: Where two small worlds meet, *Science*, 314 (2006), 1107–1110
- 2 R. Krishnamoorti, R. A. Vaia, Polymer nanocomposites, *Journal of Polymer Science Part B-Polymer Physics*, 45 (2007), 3252–3256
- 3 J. Spanoudakis, R. J. Young, Crack-propagation in a glass particle-filled epoxy-resin. 2. Effect of particle matrix adhesion, *Journal of Materials Science*, 19 (1984), 487–496
- 4 A. C. Moloney, H. H. Kausch, T. Kaiser, H. R. Beer, Parameters determining the strength and toughness of particulate filled epoxide-resins, *Journal of Materials Science*, 22 (1987), 381–393
- 5 M. Hussain, Y. Oku, A. Nakahira, K. Niihara, Effects of wet ball-milling on particle dispersion and mechanical properties of particulate epoxy composites, *Materials Letters*, 26 (1996), 177–184
- 6 E. P. Giannelis, Polymer-layered silicate nanocomposites: Synthesis, properties and applications, *Applied Organometallic Chemistry*, 12 (1998), 675–680
- 7 T. Lan, T. J. Pinnavaia, Clay-reinforced epoxy nanocomposites, *Chemistry of Materials*, 6 (1994), 2216–2219
- 8 A. S. Zerda, A. J. Lesser, Intercalated clay nanocomposites: Morphology, mechanics, and fracture behavior, *Journal of Polymer Science Part B-Polymer Physics*, 39 (2001), 1137–1146
- 9 R. P. Singh, M. Zhang, D. Chan, Toughening of a brittle thermosetting polymer: Effects of reinforcement particle size and volume fraction, *Journal of Materials Science*, 37 (2002), 781–788
- 10 R. A. Pearson, A. F. Yee, Influence of particle-size and particle-size distribution on toughening mechanisms in rubber-modified epoxies, *Journal of Materials Science*, 26 (1991), 3828–3844

- ¹¹ C. B. Bucknall, G. Maistros, C. M. Gomez, I. K. Partridge, Elastomers and thermoplastics as modifiers for thermosetting resins, *Makromolekulare Chemie-Macromolecular Symposia*, 70-1 (1993), 255–264
- ¹² R. A. Pearson, Toughening epoxies using rigid thermoplastic particles – a review, *Advances in Chemistry*, vol. 233, American Chemical Society, 1993, 405–425
- ¹³ A. C. Moloney, H. H. Kausch, H. R. Stieger, The fracture of particulate filled epoxide-resins, *Journal of Materials Science*, 19 (1984), 1125–1130
- ¹⁴ M. Frounchi, T. A. Westgate, R. P. Chaplin, R. P. Burford, Fracture of polymer networks based on diethylene glycol bis(allyl carbonate), *Polymer*, 35 (1994), 5041–5045
- ¹⁵ F. Stricker, Y. Thomann, R. Mulhaupt, Influence of rubber particle size on mechanical properties of polypropylene-SEBS blends, *Journal of Applied Polymer Science*, 68 (1998), 1891–1901
- ¹⁶ R. T. Quazi, S. N. Bhattacharya, E. Kosior, The effect of dispersed paint particles on the mechanical properties of rubber toughened polypropylene composites, *Journal of Materials Science*, 34 (1999), 607–614
- ¹⁷ A. Boonyapookana, K. Nagata, Y. Mutoh, Fatigue crack growth behavior of silica particulate reinforced epoxy resin composite, *Composites Science and Technology*, 71 (2011), 1124–1131
- ¹⁸ S. V. Kamat, J. P. Hirth, R. Mehrabian, Mechanical-properties of particulate-reinforced aluminium matrix composites, *Acta Metallurgica*, 37 (1989), 2395–2402
- ¹⁹ F. F. Lange, K. C. Radford, Fracture energy of an epoxy composite system, *Journal of Materials Science*, 6 (1971), 1197–1205
- ²⁰ A. G. Evans, Strength of brittle materials containing second phase dispersions, *Philosophical Magazine*, 26 (1972), 1327–1333
- ²¹ A. F. Bower, M. Ortiz, An analysis of crack trapping by residual-stresses in brittle solids, *Journal of Applied Mechanics-Transactions of the Asme*, 60 (1993), 175–182
- ²² A. Moiala, Q. Li, I. A. Kinloch, A. H. Windle, Thermal and electrical conductivity of single- and multi-walled carbon nanotube-epoxy composites, *Composites Science and Technology*, 66 (2006), 1285–1288
- ²³ M. Darbandi, R. Thomann, T. Nann, Hollow silica nanospheres: In situ, semi-in situ, and two-step synthesis, *Chemistry of Materials*, 19 (2007), 1700–1703
- ²⁴ W. Stober, A. Fink, E. Bohn, Controlled growth of monodisperse silica spheres in micron size range, *Journal of Colloid and Interface Science*, 26 (1968), 62–71
- ²⁵ M. Zorko, S. Novak, M. Gaberscek, Fast fabrication of mesoporous SiC with high and highly ordered porosity from ordered silica templates, *Journal of Ceramic Processing Research*, 12 (2011), 654–659
- ²⁶ I. Jerman, M. Kozelj, B. Orel, The effect of polyhedral oligomeric silsesquioxane dispersant and low surface energy additives on spectrally selective paint coatings with self-cleaning properties, *Solar Energy Materials and Solar Cells*, 94 (2010), 232–245
- ²⁷ Y. H. Lai, M. C. Kuo, J. C. Huang, M. Chen, On the PEEK composites reinforced by surface-modified nano-silica, *Materials Science and Engineering A*, 458 (2007), 158–169
- ²⁸ E. Moncada, R. Quijada, J. Retuert, Nanoparticles prepared by the sol-gel method and their use in the formation of nanocomposites with polypropylene, *Nanotechnology*, 18 (2007) 33, 335606
- ²⁹ F. Yang, G. L. Nelson, Polymer/silica nanocomposites prepared via extrusion, *Polymers for Advanced Technologies*, 17 (2006), 320–326
- ³⁰ M. Tanahashi, M. Hirose, Y. Watanabe, J. C. Lee, K. Takeda, Silica/perfluoropolymer nanocomposites fabricated by direct melt-compounding: A novel method without surface modification on nano-silica, *Journal of Nanoscience and Nanotechnology*, 7 (2007), 2433–2442
- ³¹ M. Avella, F. Bondioli, V. Cannillo, M. E. Errico, A. M. Ferrari, B. Focher, M. Malinconico, T. Manfredini, M. Montorsi, Preparation, characterisation and computational study of poly(epsilon-caprolactone) based nanocomposites, *Materials Science and Technology*, 20 (2004), 1340–1344
- ³² M. Iijima, M. Tsukada, H. Kamiya, Effect of surface interaction of silica nanoparticles modified by silane coupling agents on viscosity of methylethylketone suspension, *Journal of Colloid and Interface Science*, 305 (2007), 315–323
- ³³ M. Marrone, T. Montanari, G. Busca, L. Conzatti, G. Costa, M. Castellano, A. Turturro, A Fourier transform infrared (FTIR) study of the reaction of triethoxysilane (TES) and bis 3-triethoxysilyl-propyl tetrasulfane (TESPT) with the surface of amorphous silica, *Journal of Physical Chemistry B*, 108 (2004), 3563–3572
- ³⁴ M. Conradi, M. Zorko, I. Jerman, B. Orel, I. Verpoest, Mechanical properties of high density packed silica/poly(vinyl chloride) composites, *Polymer Engineering & Science*, (2012), DOI: 10.1002/pen.23412
- ³⁵ I. Jerman, M. Mihelcic, D. Verhovsek, J. Kovac, B. Orel, Polyhedral oligomeric silsesquioxane trisilanols as pigment surface modifiers for fluoropolymer based Thickness Sensitive Spectrally Selective (TSSS) paint coatings, *Solar Energy Materials and Solar Cells*, 95 (2011), 423–431
- ³⁶ L. Huber, B. V. Jose, *Handbook of plastics analysis*, Marcel Dekker, New York 2003
- ³⁷ X. Y. Ling, I. Y. Phang, G. J. Vancso, J. Huskens, D. N. Reinhoudt, Stable and Transparent Superhydrophobic Nanoparticle Films, *Langmuir* 25 (2009), 3260–3263
- ³⁸ M. Conradi, M. Zorko, A. Kocijan, I. Verpoest, Mechanical properties of epoxy composites reinforced with a low volume fraction of nanosilica fillers, *Materials Chemistry and Physics*, 137 (2013), 910–915
- ³⁹ J. P. Benthem, W. T. Koiter, Asymptotic approximations to crack problems, Ed., G. C. Sih, *Methods of Analysis and Solutions of Crack Problems*, Noordhoff International Publishing, Leyden 1973
- ⁴⁰ X. H. Li, G. M. Chen, Y. M. Ma, L. Feng, H. Z. Zhao, L. Jiang, F. S. Wang, Preparation of a super-hydrophobic poly(vinyl chloride) surface via solvent-nonsolvent coating, *Polymer*, 47 (2006), 506–509
- ⁴¹ T. Tamai, Y. Matsuura, M. Watanabe, K. Matsukawa, Acrylic polymer/silica hybrid for electron-beam resists, *Journal of Polymer Science, Part A: Polymer Chemistry*, 44 (2006), 2107–2116
- ⁴² Y. Y. Yu, C. Y. Chen, W. C. Chen, Synthesis and characterization of organic – inorganic hybrid thin films from poly(acrylic) and monodispersed colloidal silica, *Polymer*, 44 (2003), 593–601
- ⁴³ Y. Y. Sun, Z. Q. Zhang, K. S. Moon, C. P. Wong, Glass transition and relaxation behavior of epoxy nanocomposites, *Journal of Polymer Science Part B-Polymer Physics*, 42 (2004), 3849–3858
- ⁴⁴ J. D. Cho, H. T. Ju, Y. S. Park, J. W. Hong, Kinetics of cationic photopolymerizations of UV-curable epoxy-based SU8-negative photoresists with and without silica nanoparticles, *Macromolecular Materials and Engineering*, 291 (2006), 1155–1163
- ⁴⁵ M. Conradi, A. Kocijan, M. Zorko, I. Jerman, Effect of silica/PVC composite coatings on steel-substrate corrosion protection, *Progress in Organic Coatings*, 75 (2012), 392-397
- ⁴⁶ J. Mardel, S. J. Garcia, P. A. Corrigan, T. Markley, A. E. Hughes, T. H. Muster, D. Lau, T. G. Harvey, A. M. Glenn, P. A. White, S. G. Hardin, C. Luo, X. Zhou, G. E. Thompson, J. M. C. Mol, The characterisation and performance of Ce(dbp)(3)-inhibited epoxy coatings, *Progress in Organic Coatings*, 70 (2011), 91–101
- ⁴⁷ I. Marabotti, A. Morelli, L. M. Orsini, E. Martinelli, G. Galli, E. Chiellini, E. M. Lien, M. E. Pettitt, M. E. Callow, J. A. Callow, S. L. Conlan, R. J. Mutton, A. S. Clare, A. Kocijan, C. Donik, M. Jenko, Fluorinated/siloxane copolymer blends for fouling release: chemical characterisation and biological evaluation with algae and barnacles, *Biofouling*, 25 (2009), 481–493